

Electromagnetic Scattering by Multi-Spheres Systems and Its Application for Calculating Rain Attenuation

Nguyen Tien Dong ¹, Masahiro Tanaka ¹, Kazuo Tanaka ¹

¹ Department of Information Science, Gifu University

1-1 Yanagido, Gifu 501-1193, JAPAN

Email: dong@tnk.info.gifu-u.ac.jp

1. Introduction

The attenuation by rain has received much attention [1]–[3] since it is closely related to the quality of communication systems. With the increasing deployment of the higher frequencies in commercial wireless networks, the accurate estimation of the rain attenuation is very important for the reliable design of a radio communication system. Since the attenuation is caused by scattering and absorption of electromagnetic waves by small raindrops, the multiple scattering must be considered, especially at high frequencies. In this paper, raindrops are approximated as spheres, we can use the advantages of the analysis method to derive exact calculation of the extinction cross section. The specific rain attenuation in dB/km as a function of temperature, frequency and rainfall intensity will be derived.

Section 2 describes the analysis method. Numerical results and discussion are shown in Section 3. Section 4 is the conclusion.

2. Analysis Method

2.1 Formulation of problem

We solve electromagnetic scattering problem of a multi-sphere system with N_s spheres, each characterized by a normalized radius $x^i = \tilde{k}a^i$, a relative refractive index m^i , and a normalized position $O^i(X^i, Y^i, Z^i)$ in the global coordinates $OXYZ$, where $\tilde{k} = 2\pi/\lambda$ is the wave number, λ is the incident wavelength in the surrounding medium. We use harmonic time dependence $\exp(-i\omega t)$ for all field quantities, where ω is the circular frequency, $i = \sqrt{-1}$. In O^i coordinate system centered on sphere i , the expansion of incident, scattered and internal fields are given by

$$\mathbf{E}_{inc}^i = -E_0 \sum_{n=1}^{\infty} \sum_{m=-n}^n i^{n+1} [p_{mn}^i \tilde{\mathbf{N}}_{mn}^{(1)i} + q_{mn}^i \tilde{\mathbf{M}}_{mn}^{(1)i}], \quad (1)$$

$$\mathbf{E}_{sca}^i = E_0 \sum_{n=1}^{\infty} \sum_{m=-n}^n i^{n+1} E_{mn} [a_{mn}^i \tilde{\mathbf{N}}_{mn}^{(3)i} + b_{mn}^i \tilde{\mathbf{M}}_{mn}^{(3)i}], \quad (2)$$

$$\mathbf{E}_{int}^i = -E_0 \sum_{n=1}^{\infty} \sum_{m=-n}^n i^{n+1} [d_{mn}^i \tilde{\mathbf{N}}_{mn}^{(1)i,int} + c_{mn}^i \tilde{\mathbf{M}}_{mn}^{(1)i,int}], \quad (3)$$

where (p_{mn}^i, q_{mn}^i) , (a_{mn}^i, b_{mn}^i) and (d_{mn}^i, c_{mn}^i) are the expansion coefficients for the incident, scattered and internal fields, respectively, where E_0 is the magnitude of the incident wave. The normalized vector spherical harmonics $\tilde{\mathbf{N}}_{mn}^{(J)i}$ and $\tilde{\mathbf{M}}_{mn}^{(J)i}$, which are the abbreviation of $\tilde{\mathbf{M}}_{mn}^{(J)}(\rho, \theta, \phi)$ and $\tilde{\mathbf{N}}_{mn}^{(J)}(\rho, \theta, \phi)$, are defined by

$$\tilde{\mathbf{M}}_{mn}^{(J)} = [\hat{\mathbf{e}}_{\theta} i \tilde{\pi}_{mn}(\theta) - \hat{\mathbf{e}}_{\phi} \tilde{\tau}_{mn}(\theta)] z_n^{(J)}(\rho) \exp(im\phi), \quad (4)$$

$$\tilde{\mathbf{N}}_{mn}^{(J)} = \left\{ \hat{\mathbf{e}}_r n(n+1) \tilde{P}_n^m(\cos\theta) \frac{z_n^{(J)}(\rho)}{\rho} + [\hat{\mathbf{e}}_{\theta} \tilde{\tau}_{mn}(\theta) + \hat{\mathbf{e}}_{\phi} i \tilde{\pi}_{mn}(\theta)] \frac{[\rho z_n^{(J)}(\rho)]'}{\rho} \right\} \exp(im\phi), \quad (5)$$

where $\hat{\mathbf{e}}_r, \hat{\mathbf{e}}_{\theta}, \hat{\mathbf{e}}_{\phi}$ are the unit vectors in the spherical coordinates, $z_n^{(J)}$ is the appropriate kinds of spherical Bessel or Hankel function $j_n, y_n, h_n^{(1)}$, and $h_n^{(2)}$, for $J = 1, 2, 3$, and 4, respectively; we use only the value

of $J = 1$ and $J = 3$ in our work. The prime denotes differentiation with respect to argument. The functions $\tilde{\pi}_{mn}(\theta)$ and $\tilde{\tau}_{mn}(\theta)$ are defined by

$$\tilde{\pi}_{mn}(\theta) = \frac{m}{\sin \theta} \tilde{P}_n^m(\cos \theta), \quad \tilde{\tau}_{mn}(\theta) = \frac{d}{d\theta} \tilde{P}_n^m(\cos \theta), \quad \tilde{P}_n^m = \left[\frac{(2n+1)(n-m)!}{n(n+1)(n+m)!} \right]^{1/2} P_n^m, \quad (6)$$

where \tilde{P}_n^m and P_n^m are the normalized and conventional associated Legendre functions without phase factor $(-1)^m$, respectively.

2.1.1 Incident coefficients

Without loss of generality, the incident plane wave vector always points to the positive z direction. The incident wave has a linear polarization angle α_p and is characterized by the wave vector $\tilde{\mathbf{k}}_{inc} = \tilde{k} \hat{\mathbf{e}}_z$, where $\hat{\mathbf{e}}_z$ together with $\hat{\mathbf{e}}_x, \hat{\mathbf{e}}_y$ are the orthonormal unit vectors in the Cartesian coordinate system.

$$p_{mn}^i = \exp(i\tilde{k}Z^i) m \delta_{|m|,1} \frac{\sqrt{2n+1}}{2} \exp(-im\alpha_p), \quad q_{mn}^i = -\exp(i\tilde{k}Z^i) \delta_{|m|,1} \frac{\sqrt{2n+1}}{2} \exp(-im\alpha_p), \quad (7)$$

where Kronecker delta $\delta_{|m|,1} = 1$ if $|m| = 1$ and $\delta_{|m|,1} = 0$ if $|m| \neq 1$.

2.1.2 Scattered coefficients

By using the superposition of Mie theory, scattered electric field of sphere i can be expressed as

$$\mathbf{E}_{sca}^i = \mathcal{M} \left(\mathbf{E}_{inc}^i + \sum_{\substack{j=1 \\ j \neq i}}^{N_s} \mathbf{E}_{sca}^j \right), \quad (8)$$

where the symbol \mathcal{M} denotes the application of Mie theory. The Mie coefficients for sphere i depend on the normalized radius x^i and the relative refractive index m^i as

$$\alpha_n^i = \frac{m^i \psi_n'(x^i) \psi_n(m^i x^i) - \psi_n(x^i) \psi_n'(m^i x^i)}{m^i \xi_n'(x^i) \psi_n(m^i x^i) - \xi_n(x^i) \psi_n'(m^i x^i)}, \quad \beta_n^i = \frac{\psi_n'(x^i) \psi_n(m^i x^i) - m^i \psi_n(x^i) \psi_n'(m^i x^i)}{\xi_n'(x^i) \psi_n(m^i x^i) - m^i \xi_n(x^i) \psi_n'(m^i x^i)}, \quad (9)$$

where $\psi_n(z) = z j_n(z)$ and $\xi_n(z) = z h_n^{(1)}(z)$, j_n and $h_n^{(1)}$ are the spherical Bessel and Hankel functions of the first kind, respectively.

Imposing the standard boundary condition for electromagnetic fields at the surface of each sphere gives a set of inhomogeneous linear equation for the coefficients (a_{mn}^i, b_{mn}^i)

$$a_{mn}^i = \alpha_n^i \left[p_{mn}^i - \sum_{\substack{j=1 \\ j \neq i}}^{N_s} \sum_{l=1}^{\infty} \sum_{k=-l}^l (A_{mn}^{kl} a_{kl}^j + B_{mn}^{kl} b_{kl}^j) \right], \quad b_{mn}^i = \beta_n^i \left[q_{mn}^i - \sum_{\substack{j=1 \\ j \neq i}}^{N_s} \sum_{l=1}^{\infty} \sum_{k=-l}^l (A_{mn}^{kl} b_{kl}^j + B_{mn}^{kl} a_{kl}^j) \right], \quad (10)$$

where (a_{mn}^i, b_{mn}^i) are scattered coefficients, (p_{mn}^i, q_{mn}^i) are incident coefficients, (α_n^i, β_n^i) are Mie coefficients for sphere i , $(A_{mn}^{kl}, B_{mn}^{kl})$ are addition coefficients. The addition theorems for vector spherical harmonics, which transform harmonics from one coordinate system into another are used to calculate the addition coefficients [4].

2.1.3 Internal coefficients

The internal coefficients (d_{mn}^i, c_{mn}^i) are related to the scattering coefficients by

$$d_{mn}^i = \frac{im^i}{m^i \psi_n'(x^i) \psi_n(m^i x^i) - \psi_n(x^i) \psi_n'(m^i x^i)} a_{mn}^i, \quad c_{mn}^i = \frac{im^i}{\psi_n'(x^i) \psi_n(m^i x^i) - m^i \psi_n(x^i) \psi_n'(m^i x^i)} b_{mn}^i. \quad (11)$$

2.2 Total cross sections

Total scattering, extinction and absorption cross sections of the configuration are given by

$$C_{ext} = \frac{4\pi}{\tilde{k}^2} \text{Re} \sum_{i=1}^{N_s} \sum_{n=1}^{\infty} \sum_{m=-n}^n (a_{mn}^i p_{mn}^{i*} + b_{mn}^i q_{mn}^{i*}), \quad (12)$$

$$C_{sca} = \frac{4\pi}{\tilde{k}^2} \text{Re} \sum_{i=1}^{N_s} \sum_{n=1}^{\infty} \sum_{m=-n}^n (a_{mn}^{i*} a_{mn}^{Ti} + b_{mn}^{i*} b_{mn}^{Ti}), \quad (13)$$

$$C_{abs} = \frac{4\pi}{\tilde{k}^2 |m^i|^2} \text{Re} \sum_{i=1}^{N_s} \sum_{n=1}^{\infty} \sum_{m=-n}^n i \psi'_n(m^i x^i) \psi_n^*(m^i x^i) \times (m^{i*} |d_{mn}^i|^2 + m^i |c_{mn}^i|^2), \quad (14)$$

where the asterisk denotes complex conjugate and

$$a_{mn}^{Ti} = \sum_{j=1}^{N_s} \sum_{l=1}^{\infty} \sum_{k=-l}^l (a_{kl}^j \tilde{A}_{mn}^{kl} + b_{kl}^j \tilde{B}_{mn}^{kl}), \quad b_{mn}^{Ti} = \sum_{j=1}^{N_s} \sum_{l=1}^{\infty} \sum_{k=-l}^l (a_{kl}^j \tilde{B}_{mn}^{kl} + b_{kl}^j \tilde{A}_{mn}^{kl}), \quad (15)$$

where \tilde{A}_{mn}^{kl} , \tilde{B}_{mn}^{kl} coefficients are calculated as A_{mn}^{kl} , B_{mn}^{kl} , but with spherical Hankel function $h_n^{(1)}$ replaced by spherical Bessel function j_n .

3. Numerical Results and Discussions

Since the refractive index of raindrops depends on temperature and electromagnetic frequency [5], and the properties (number, size, position) of raindrops in the unit volume depend on the rainfall intensity and the raindrop distribution model (we use Weibull distribution model [6] in this paper), the specific rain attenuation γ in dB/km caused by scattering and absorption of electromagnetic waves by raindrops depends on the temperature, frequency and rainfall intensity.

In Weibull distribution model, the radius of N_s sampled raindrops are given

$$a_i = \psi \{-\log [1 - (i - 1/2) N_s]\}^{1/\eta}, \quad (16)$$

where $\psi = 0.13R^{0.44}$ and $\eta = 0.95R^{0.14}$. We suppose that N_s raindrops are randomly distributed inside a fictitious sphere having the volume $V[\text{m}^3] = N_s/N_0$, where $N_0 = 1000[\text{m}^{-3}]$.

Since $C_{ext} = C_{sca} + C_{abs}$, the specific rain attenuation depends on the extinction cross section by

$$\gamma[\text{dB/km}] = \frac{C_{ext}}{V} \times 10^3 \times \log_{10} e = 4343 \frac{C_{ext}}{V}. \quad (17)$$

Figure 1 shows the behavior of rain attenuation for several parameters (note that the minus temperature implies super cooled water, not ice). When the temperature increases, the attenuation is almost constant at low frequencies ($f < 30\text{GHz}$) and slightly decreases at higher frequencies (see Figure 1(a,b)). When the rainfall intensity increases, the attenuation increases, especially at the higher frequencies (see Figure 1(c)). The attenuation also increases when the number of sampled raindrops increases (see Figure 1(d)). It means we should increase the number of sampled raindrops to get the exact value of attenuation.

4. Conclusion

Exact solution of electromagnetic scattering by multi-sphere system has been developed to the problem of calculating specific rain attenuation. We also investigate the relation of rain attenuation with temperature of the environment, frequency of the electromagnetic wave and the rainfall intensity using Weibull distribution formula. The present results and discussions will become more convincing if we deal with raindrops of realistic shape and incident wave.

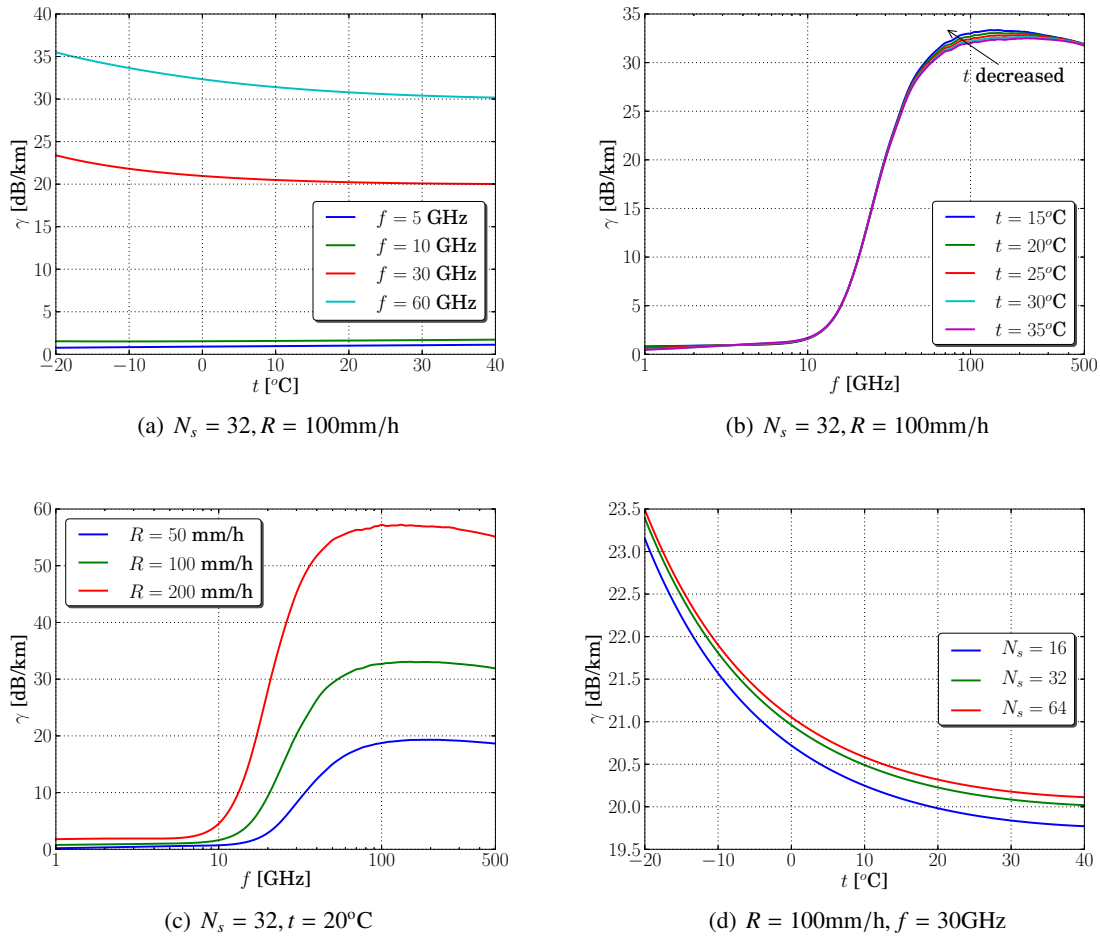


Figure 1: Dependence of specific rain attenuation γ on (a) temperature t , (b) frequency f , (c) rainfall intensity R and (d) number of sampled raindrops N_s .

References

- [1] E. Setijadi, A. Matsushima, N. Tanaka, and G. Hendranto, "Effect of temperature and multiple scattering on rain attenuation of electromagnetic waves by a simple spherical model," *Progress In Electromagnetics Research*, vol.99, pp.339–354, 2009.
- [2] M. Bahrami, J. Rashed-Mohassel, and M. Mohammad-Taheri, "An exact solution of coherent wave propagation in rain medium with realistic raindrop shapes," *Progress In Electromagnetics Research*, vol.79, pp.107–118, 2008.
- [3] S. Kanellopoulos, A. Panagopoulos, and J. Kanellopoulos, "Calculation of electromagnetic scattering from a pruppacher-pitter raindrop using m.a.s. and slant path rain attenuation prediction," *International Journal of Infrared and Millimeter Waves*, vol.26, no.12, pp.1783–1802, 2005.
- [4] N.T. Dong, M. Tanaka, and K. Tanaka, "Improved Algorithms for Calculating Addition Coefficients in Electromagnetic Scattering by Multi-Sphere Systems," *IEICE Trans. Electron.*, vol.E95-C, no.1, pp.27–35, 2012.
- [5] T. Meissner and F. Wentz, "The complex dielectric constant of pure and sea water from microwave satellite observations," *IEEE Trans Geosci Remote Sens.*, vol.42, pp.1836–1849, 2004.
- [6] M. Sekine, C.D. Chen, and T. Musha, "Rain attenuation from log-normal and Weibull raindrop-size distributions," *IEEE Trans. on Antennas and Propagation*, vol.35, no.3, pp.358–359, 1987.